

MAX-PLANCK-INSTITUT FÜR PHYSIK
(WERNER-HEISENBERG-INSTITUT)

Report to the Fachbeirat

2007 – 2010

Part II: Scientific Achievements

Cover Photo:

The cover photo shows two crystals to be used for the CRESST (Cryogenic Rare Event Search with Superconducting Thermometers) experiment located at the Laboratori Nazionali del Gran Sasso (LNGS) in Italy. The CRESST experiment is designed for direct detection of weakly interacting massive particles, accounting for the dark matter observed in the universe. The Max-Planck-Institut für Physik is substantially contributing to all essential aspects of the experiment.

Contents

- 0.1 ATLAS Physics Analysis 3
 - 0.1.1 Standard Model Processes 3
 - 0.1.2 Top-Quark Physics 5
 - 0.1.3 Searches for the Higgs Boson 10
 - 0.1.4 Search for Physics Beyond the Standard Model 14
 - 0.1.5 Analyses Summary 17

0.1 ATLAS Physics Analysis

For a long time the MPP ATLAS group has been continuously working on the preparation of physics analysis of hadron collision data at the LHC. The results obtained in the years 1997-2007, including preparatory work based on Tevatron data, are described in the previous reports [?] (p.82-84), [?] (p.106-112), [?], and references therein.

The present physics studies for the ATLAS experiment cover a broad physics range. Already at the early stage of data taking, a number of Standard Model (SM) processes occur in abundance. These processes allow for detailed studies of the detector performance, as well as for the precision measurement of QCD and electroweak observables. The data collected so far allow for the first measurements of inclusive lepton distributions, as well as the observation of electroweak gauge bosons. Also the processes involving top-quarks will very soon become measurable as the integrated luminosity increases. A good understanding of SM processes is essential also for new discoveries. The ATLAS discovery potential is explored in searches for the Higgs boson both in the Standard Model and in supersymmetric extensions, as well as in a generic search for supersymmetric particles and other phenomena like the lepton flavour violation. The ongoing investigations are described in more detail below.

0.1.1 Standard Model Processes

Inclusive Lepton Cross Sections

At the LHC pp collision events with highly energetic electrons and muons in the final state provide clean signatures for many physics processes of interest. A good understanding of the inclusive electron and muon cross sections is therefore of great importance. The MPP group contributes to these measurements [?, ?, ?].

At the LHC electrons are produced predominantly in decays of heavy quarks for transverse energies below about 30 GeV and in decays of W and Z bosons at higher transverse energies. The MPP group significantly contributed to the optimization of the electron selection criteria to arrive at an electron selection efficiency which is flat in the transverse electron energy (see Fig. 1). The first measured inclusive electrons spectrum at a center of mass energy of 7 TeV at the LHC is shown in Fig. 2 in comparison with the prediction of the Pythia minimum bias Monte-Carlo. The

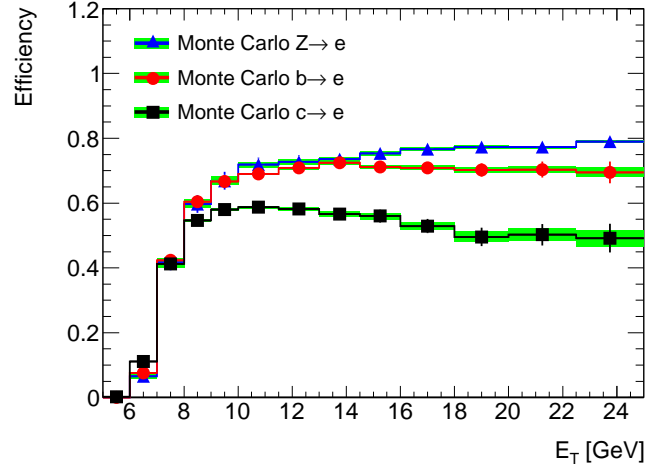


Figure 1: Monte-Carlo prediction of the electron reconstruction efficiency for electrons from heavy quark and Z boson decays. [?]

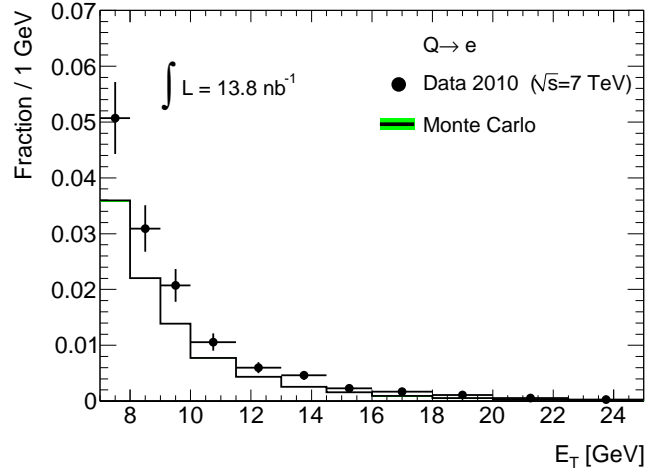


Figure 2: Comparison of the measured distribution of the transverse energies of prompt electrons from c and b decays with the Pythia 6.4 minimum bias Monte-Carlo predictions. [?]

MPP group contributes to the study of the observed 20% discrepancy between data and Monte-Carlo prediction, using the increasing statistics of the inclusive electron sample.

The MPP group is also involved in the measurement of the inclusive muon cross section contributing with its experience in muon performance studies. The measured inclusive muon p_T spectrum is presented in Fig. 3 where it is compared to the Pythia 6.4 minimum bias Monte-Carlo prediction. The measured spectrum is well reproduced by the Monte-Carlo simulation. The discrepancy observed for $p_T > 20$ GeV is due to muons originating from W and Z boson decays. According to the Monte-Carlo simulation, the

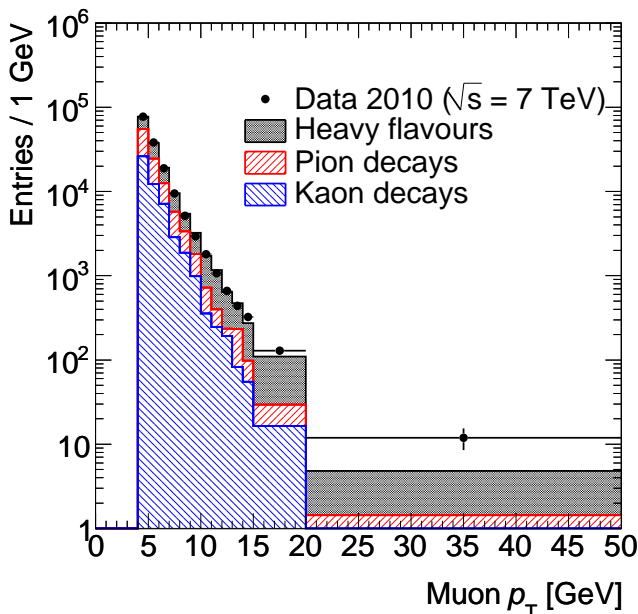


Figure 3: Comparison of the measured inclusive muon transverse momentum spectrum with the Pythia 6.4 minimum bias Monte-Carlo prediction. The Monte-Carlo data is decomposed into three sources of muons, namely in-flight decays of charged pions and kaons and the decays of heavy-flavour hadrons. [?]

main sources of muons at transverse momenta below 20 GeV are in-flight decays of charged pions and kaons and the decays of heavy-flavour hadrons. The contribution of pion and kaon decays in-flight to the inclusive muon spectrum will be estimated from data by comparing the momentum measured in the inner detector with the momentum measured in the muon spectrometer. Late pion and kaon decays in the inner detector lead to a large momentum imbalance between the inner detector and muon spectrometer as illustrated in Fig. 4, as the inner detector measures the pion or kaon momentum while the muon spectrometer measures the momentum of the decay muon.

Electroweak Gauge Boson Production

The measurement of the W and Z boson production is a first essential step in understanding hard electroweak processes in the high-energy regime of the LHC. With a sufficient amount of collected data, precise inclusive and differential cross section measurements can be performed to probe the parton density functions. In addition, these processes are studied with the motivation of estimating the backgrounds to the searches for Higgs bosons and supersymmetric particles. Of particular interest here is the electroweak gauge bosons

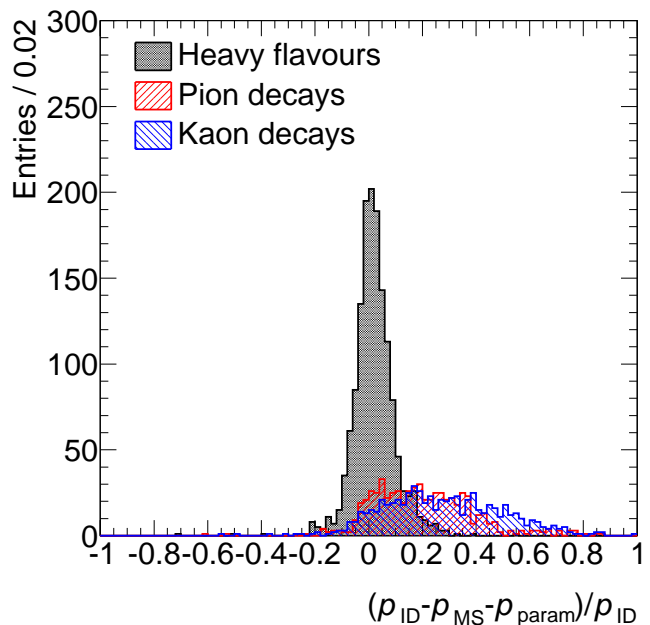


Figure 4: Distribution of the difference of the muon momentum measurements in the inner detector and the muon spectrometer normalized to the inner detector momentum measurements in simulated data. [?]

production in association with jets, where the bosons are decaying into electrons, muons or τ leptons.

W bosons have already been observed in the first 16.6 nb^{-1} of pp collision data collected with ATLAS: 43 W bosons in the $e\nu_e$ final state and 67 W boson in the $\mu\nu_\mu$ final state. As expected for pp collisions, more W^+ than W^- bosons have been detected, 70 W^+ and 40 W^- bosons. The first measurements of inclusive W and Z production cross-sections have also been performed. Fig. 5 shows the transverse mass distribution of the $W \rightarrow \mu\nu_\mu$ candidates in the first 16.6 nb^{-1} of pp collision data collected by ATLAS. The Monte-Carlo prediction is consistent with the measured distribution and has a negligible background contamination. A first measurement of the W production cross section could also be performed. The experimental error of the cross section is dominated by the statistical error of the number of observed W candidates and the 10% uncertainty of the luminosity measurement. The measured W production cross section agrees well with the NNLO calculations as shown in Fig. 6.

Also candidates for $Z \rightarrow \ell^+\ell^-$ decays with isolated charged leptons were observed by ATLAS. In the recently collected 229 nb^{-1} of pp collision data ATLAS observes clear Z peaks in the dilepton invariant mass spectra as shown in Fig. 7 [?]. The measured cross sections of $[0.72 \pm$

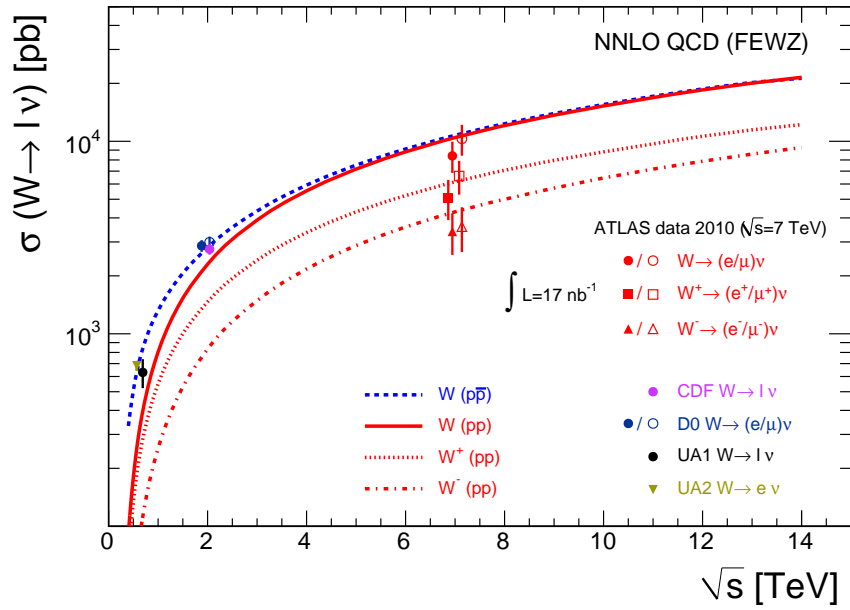
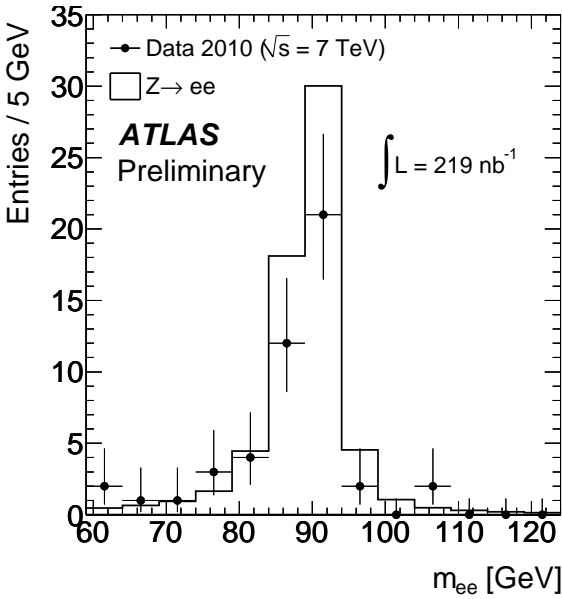
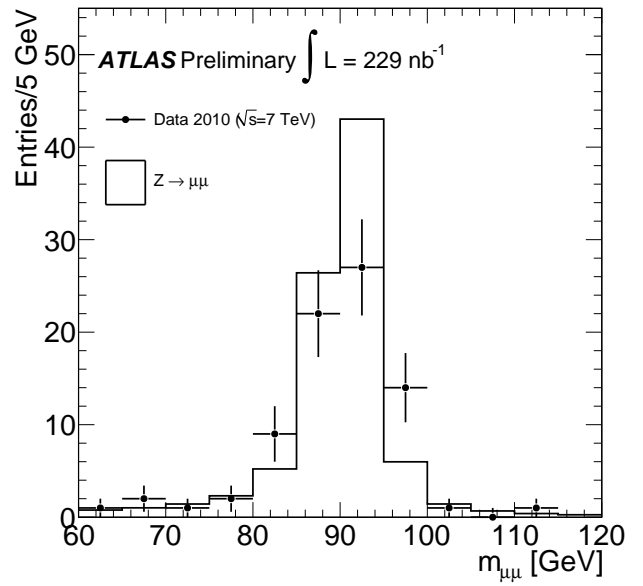


Figure 6: Comparison of the measured W cross section with the NNLO prediction. [?] The expected asymmetry in the production cross sections of W^+ and the W^- boson is confirmed by the cross section measurements.



(a)



(b)

Figure 7: Invariant mass $m_{\ell\ell}$ of Z candidates in the electron (a) and muon (b) channels. [?]

$0.11(\text{stat}) \pm 0.10(\text{syst}) \pm 0.08(\text{lumi})$ nb for $Z \rightarrow e^+e^-$ and $[0.89 \pm 0.10(\text{stat}) \pm 0.07(\text{syst}) \pm 0.10(\text{lumi})]$ nb for $Z \rightarrow \mu^+\mu^-$ are in agreement with the theoretical prediction as illustrated in Figure 8.

0.1.2 Top-Quark Physics

Overview

The top-quark is by far the heaviest known elementary building block of matter. The precise knowledge of the quantum numbers of the top-quark helps to further constrain the parameters of the Standard Model, and is a mandatory prerequisite for any study of new physics that will almost inevitably suffer from top-

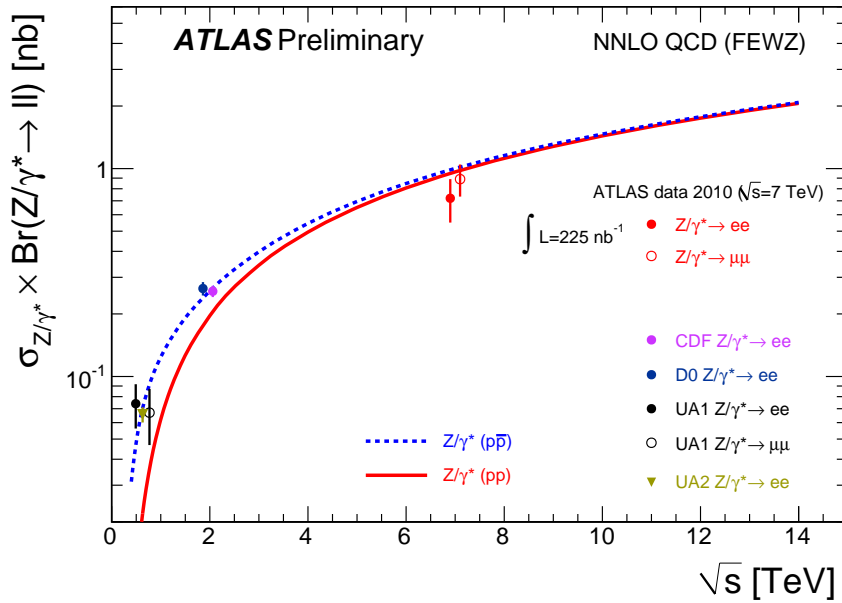


Figure 8: Comparison of the measured values of $\sigma_Z \cdot BR(Z \rightarrow \ell\ell)$ for $\ell = e, \mu$ with the theoretical predictions based on NNLO QCD calculations. [?]

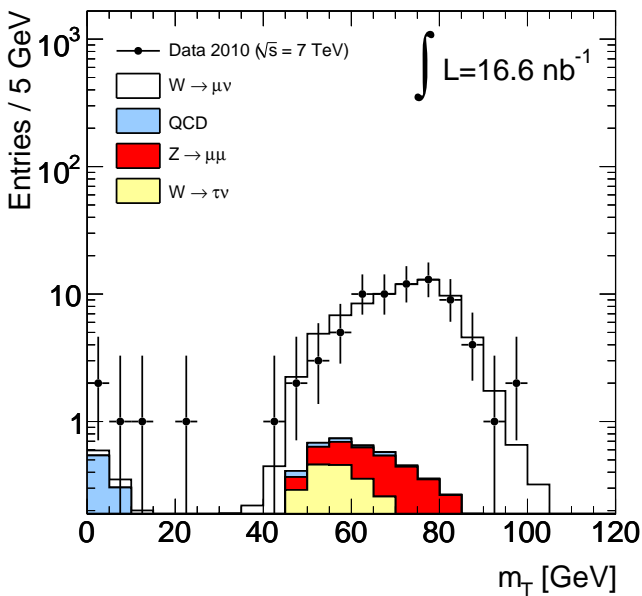


Figure 5: Transverse mass distribution of $W \rightarrow \mu\nu_\mu$ candidates found in 16.6 nb^{-1} of pp collision data collected by ATLAS. [?]

quark reactions as background processes. In addition, the top-quark should have the strongest couplings to any mechanism that generates mass, which makes it a very interesting object for an unbiased search for this mechanism.

The present main interest of the top-quark physics analysis work of the MPP group is the investigation of the $t\bar{t}$ production process, and particularly the determination of the mass of the top-quark (m_{top}) and

the production cross-section ($\sigma_{t\bar{t}}$) in the reaction $t\bar{t} \rightarrow b\bar{b}W^+W^-$.

The analyses use two decay channels of the W-boson pair, the lepton+jets channel, where the W-boson pair decays into $\ell\nu qq'$ with $\ell = e, \mu$ (branching ratio, $BR = 30\%$) and the all-jets channel, where both W-bosons decay into a qq' pair ($BR = 44\%$). In both channels m_{top} is obtained from hadronically decaying W-bosons and the corresponding b-jet.

The main background reactions to $t\bar{t}$ production, as determined from Monte Carlo simulations, are the $W+n$ -jets production, QCD multijet production, single top-quark production, and that fraction of the $t\bar{t}$ production where the W-boson pair decays via the other decay channels. The QCD multijet production process is special due to the huge cross-section before any cut, such that event samples fully covering the signal phase space cannot be simulated with sufficient statistics, especially for the lepton+jets channel, where the selected lepton mostly results from a wrongly reconstructed jet. Eventually this background contribution has to be obtained from data. So far, initial studies of this background based on Monte Carlo samples have been performed and methods to evaluate it from the data, like the matrix-method, have been implemented. The matrix-method was successfully applied to estimate the background fraction from Monte Carlo samples with a deliberately unknown composition of signal and background events [?]. In the MPP investigations, for the first time the k_T -jet algorithm has

been used in top physics analyses at ATLAS [?, ?] Because of a better stability against divergences, this algorithm is theoretically preferred over the traditionally applied cone-jet algorithm. By now also the experimental advantages became apparent, such that since recently a variant of it, namely the anti- k_t jet algorithm is the ATLAS standard.

At present the analyses are optimized on Monte Carlo samples and are ready to be applied to the data to be taken still this year. The analyses are mostly performed assuming the initially envisaged proton-proton center of mass energy of $\sqrt{s} = 10 \text{ TeV}$ and for integrated luminosities \mathcal{L}_{int} of several 100 pb^{-1} . An overview of the recent activities is given below, the initial investigations were reported in [?] (p.106-112), [?].

Lepton + Jets Channel

The lepton+jets channel is the best compromise of branching fraction and signal-to-background ratio (S/B), defined as the ratio of $t\bar{t}$ signal events to physics background events. Therefore most of the effort is invested in this channel. At MPP a number of analyses have been performed to arrive at the most sensitive observable and analysis strategy for obtaining m_{top} from the invariant mass of the three jets assigned to the decay products of the hadronically decaying top-quark. Different event- and jet selection algorithms, observables, jet calibration schemes (see Sec. ??), and fitting methods have been exploited for this.

In the lepton+jets channel the charged lepton with a high transverse momentum¹ (p_T) from the decay of one W-boson is utilized to trigger and identify the event, and to efficiently suppress background without genuine charged leptons, i.e. from the QCD multijet production. In general, the event selection for the lepton+jets channel requires an isolated electron or muon within the good acceptance of the detectors, which has a transverse momentum of more than 20 GeV and lies within the rapidity range of $|\eta| < 2.5$. Since the initial state is balanced in p_T , to account for the neutrino a missing transverse energy of more than 20 GeV is required. In addition, at least four jets are required

¹In the ATLAS right-handed coordinate system the x -axis points towards the center of the LHC ring, the y -axis points upwards and the z -axis points in the direction of the counter-clockwise running proton beam. The polar angle θ and the azimuthal angle ϕ are defined with respect to the z -axis and x -axis, respectively. The pseudo-rapidity is defined as $\eta = -\ln(\tan(\theta/2))$ and the radial distance in (η, ϕ) space is $\Delta R = \sqrt{\Delta\eta^2 + \Delta\phi^2}$.

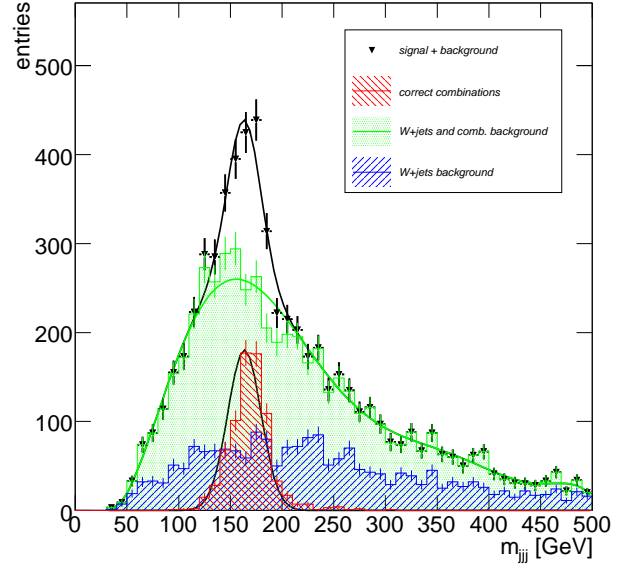


Figure 9: The reconstructed top-quark mass together with a fit.

within the same range of rapidity, and having transverse momenta of more than 40 GeV for the three highest p_T jets, and more than 20 GeV for the fourth jet. All jets should be well separated from the identified lepton. Given the different emphasis of the analyses, these requirements are slightly modified or additional requirements like the presence of identified b-jets, or restrictions to the reconstructed invariant mass of the W-boson are imposed. With these selections, for each lepton sample an average signal efficiency of about 10% is reached, and the S/B is about 1.5.

The standard assignment of jets to the top-quark and the W-Boson are as follows. For each event, from all jets with $p_T > 20 \text{ GeV}$ the three jet combination which maximizes the transverse momentum is chosen to form the hadronically decaying top-quark. This algorithm is named the p_T -max method. Out of this, the two jet pair with the smallest ΔR is taken to represent the W-boson. A typical top-quark mass spectrum observed with these requirements [?], and only using signal events and W+n-jets events, is shown in Fig. 9. In this example, the spectrum is fitted with a Gaussian function to parameterize the correct combinations leading to the top-quark mass and width, and a sum of Chebyshev polynomials used to describe the events stemming from the sum of the physics background events and wrong jet combinations in selected signal events. The Gaussian part of the fit is also shown separately and compared to the red histogram made from the correct jet triplet. In this case correct jet triplets

are defined as those combinations of jets where the reconstructed four-vector of the jet triplet coincides with that of the top-quark to within $\Delta R = 0.1$.

From this figure it is clear that firstly the correct jet triplets constitute only a small part of the events in the peak region around the generated top-quark mass of 172.5 GeV, secondly that the shape of the combinatorial background can well influence the fitted peak value, and thirdly that the shown W + n-jets contribution is still sizeable and not entirely flat.

These issues are addressed, e.g. by using other algorithms to select the jet triplet, or by exploiting additional variables or a constrained fit that both help to separate signal from background. Additional algorithms studied include the so-called ΔR method that exploits the angular correlations between the two b-jets that should have a large ΔR , and the two light-jets that should have a small ΔR . This algorithm works without explicitly using b-jet identification, instead from a p_T ordered jet list the first two jets are assumed to be the b-jets and the next two jets to stem from the W-Boson decay. On these jets the angular requirements are applied. Whether the decrease in statistical precision compared to the p_T -max method is compensated by superior features like an improved resolution, or a smaller bias in the reconstructed mass, is under investigation.

Due to the presence of the decay of the top-quarks that correlate the W-Bosons and their corresponding b-quarks, the signal events should exhibit a different correlation of the observed jet structure than the background processes without top-quarks. The separation of the jets can be monitored when running the k_T -jet algorithm by studying the $d_{\text{merge}}(M \rightarrow M - 1)$ values at which an M -jet configuration is reduced to an $(M - 1)$ -jet configuration. In a multivariate analysis it was found that the d_{merge} values in signal and background events are not sufficiently different to be used as discriminating variables [?]. In contrast, a likelihood function build from seven event variables, like e.g. the invariant mass of the charged lepton and its assigned b-jet, or the ΔR between the W-Boson and the b-jet from the hadronically decaying top-quark candidate, is clearly able to significantly improve the S/B, while retaining most of the events where the correct jet triplet was selected. This is demonstrated in Fig. 10.

A kinematic fit exploiting as constraints the known W-Boson mass both for the leptonic and the hadronic W-Boson decays, and in addition the equality of the two corresponding reconstructed top-quark masses

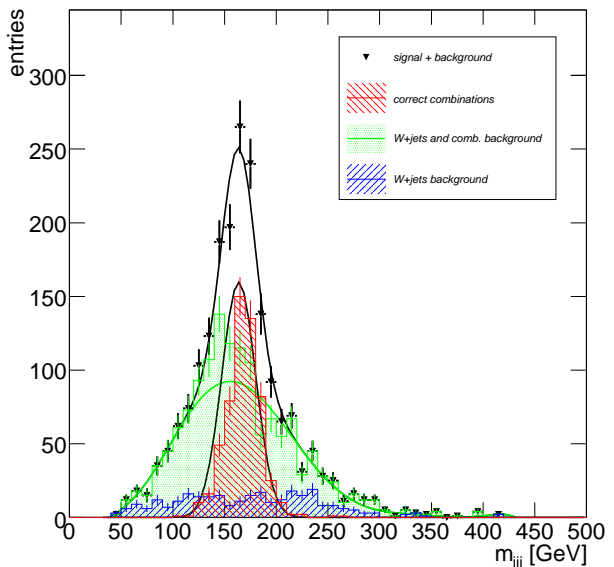


Figure 10: Same as Fig. 9 but with an additional likelihood selection.

mainly serves three purposes. Firstly, it increases the efficiency for selecting the correct jet triplet by making more detailed use of the entire event. Secondly, it provides a quality measure, namely the probability $P(\chi^2)$ of the fit, to better suppress background events. Finally, it improves on the resolution of the top-quark mass provided the uncertainties of the measured quantities and their correlations are properly understood, something that is only expected after a larger data set has been analyzed. Compared to the p_T -max method the efficiency for selecting the correct jet triplet is increased by about 15% absolute, and about 25% of the background events can be removed [?] by requiring $P(\chi^2) > 0.15$. An example of such a selection for events with four reconstructed jets and requiring $P(\chi^2) > 0.15$ is shown in Fig. 11. The better suppression of the W + n-jets events compared to Fig. 9 is apparent. It has been verified that this improvement, is very stable against variations of the assumed object resolutions. Since at the moment only initial approximations are made for the resolution of the objects, the possible improvement in the mass resolution is not yet exploited.

The largest systematic uncertainty in any determination of m_{top} stems from the imperfect knowledge of the jet energy scale (JES), which depends on kinematic properties like p_T and η of the jets, and is different for light-jets and b-jets. Therefore, one of the most important features of any m_{top} estimator is the stability against the variation of the JES. To minimize the JES

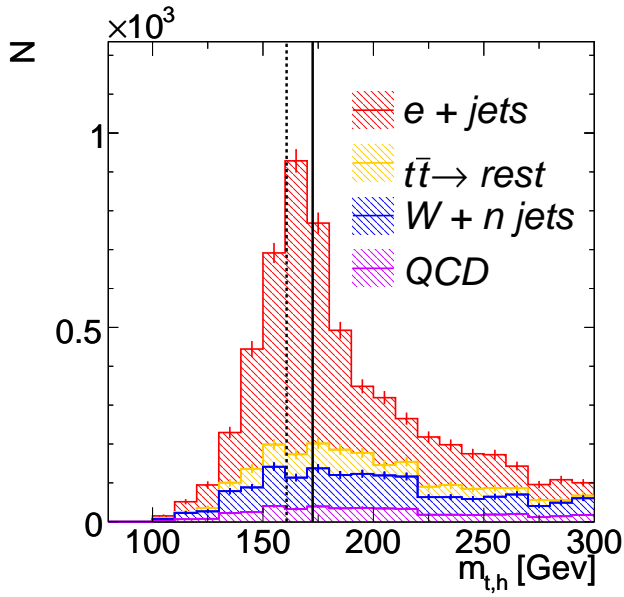


Figure 11: The top-quark mass distribution when applying a constrained fit selection.

uncertainty on the measured m_{top} two paths are followed: one is a calibration by means of the known W-boson mass ($M_{\text{W}}^{\text{PDG}}$) to obtain the JES for light-jets, the other is exploring the stabilized top-quark mass ($m_{\text{top}}^{\text{stab}}$, see below) to be as independent as possible of the actual JES value, without actually determining it.

In the lepton + jets channel an iterative in-situ calibration of the JES for the selected events has been performed [?]. Jets are treated in the massless limit with unchanged reconstructed angles, such that any change in the invariant two-jet mass ($M_{\text{W}}^{\text{reco}}$) can be expressed in energy dependent JES factors. The jet calibration then makes use of the fact that $M_{\text{W}}^{\text{reco}}$ calculated from the jets assigned to the W-boson decay has to match $M_{\text{W}}^{\text{PDG}}$. The energy bins are chosen logarithmically from 50 GeV to 400 GeV and the resulting calibration factors, which are consecutively applied per iteration, are shown in Fig. 12 for the initial situation, the 9th iteration and the final result. The flatness of the calibration factors of the 9th iteration with values close to unity clearly shows that the fit has converged. Comparing the initial and final situation reveals that the iterations slightly change the simple picture one would have obtained by once adjusting the peak of the initial distribution to $M_{\text{W}}^{\text{PDG}}$. When applying this global scaling method the uncertainty on m_{top} from the JES uncertainty is considerably reduced [?].

The variable $m_{\text{top}}^{\text{stab}}$ is calculated as the ratio of the reconstructed masses of the top-quark and the W-Boson candidates from the selected jet triplet. For conve-

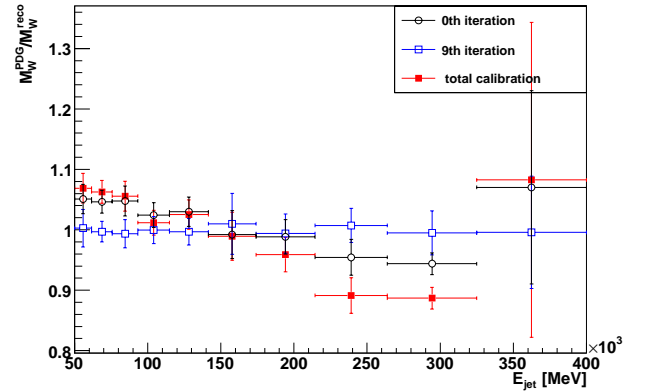


Figure 12: In-situ calibration of the W-Boson mass as function of the light-jet energy.

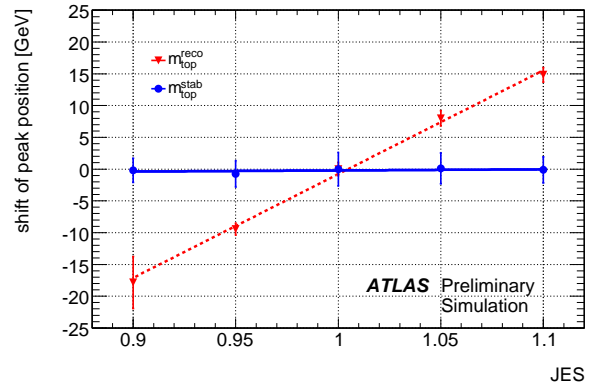


Figure 13: Stability of $m_{\text{top}}^{\text{reco}}$ and $m_{\text{top}}^{\text{stab}}$ against JES changes.

nience this ratio is multiplied by $M_{\text{W}}^{\text{PDG}}$. The main consequence of using $m_{\text{top}}^{\text{stab}}$ is a strong event-by-event cancellation of the JES dependence of the three-jet and two-jet masses in the mass ratio, while retaining the sensitivity to m_{top} . The quantitative gain in stability when using $m_{\text{top}}^{\text{stab}}$ instead of the jet triplet invariant mass $m_{\text{top}}^{\text{reco}}$ is apparent from Fig. 13 taken from [?] Using this variable a template analysis has been developed [?, ?, ?]. In this analysis Probability Density Functions (PDFs) are constructed from templates of the signal events at various assumed m_{top} values and from a template of the combined physics background events. The signal PDF linearly depends on m_{top} , whereas the background PDF does not. Using pseudo-experiments for a given luminosity the sensitivity of the method, together with the systematic uncertainties from various sources, has been estimated. An example of a pseudo experiment is shown in Fig. 14 for the muon channel and for $\sqrt{s} = 10 \text{ TeV}$ and $\mathcal{L}_{\text{int}} = 100 \text{ pb}^{-1}$. For this situation the statistical uncertainty for the combined electron and muon channel is about

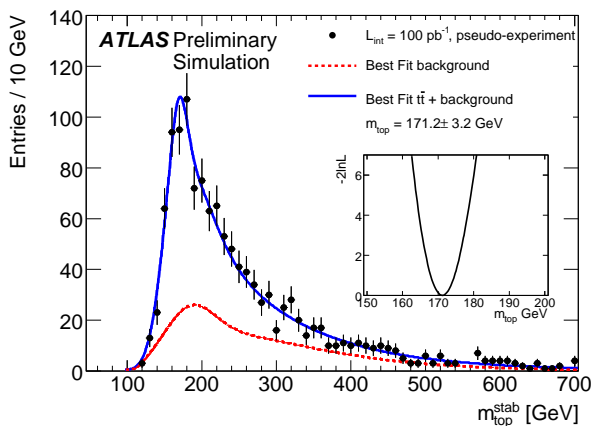


Figure 14: Pseudo-experiment mimicking early ATLAS data in the muon channel.

2 GeV. The total systematic uncertainty is estimated to be about 3.8 GeV for each channel, still dominated by the systematic uncertainty from the JES for light jets and b-jets [?].

The determination of the combinatorial- and physics background from data rather than from Monte Carlo samples likely results in a reduced systematic uncertainty. For this purpose a data driven method was developed that explores the $m_{\text{top}}^{\text{reco}}$ and $R_{\text{top}} = m_{\text{top}}^{\text{reco}}/M_{\text{W}}^{\text{reco}}$ distributions at the same time. The idea is to use e.g. the events from the sideband region of the $m_{\text{top}}^{\text{reco}}$ distribution to predict the shape of the background contribution to the R_{top} distribution. An initial investigation ignoring possible shape differences of the combinatorial- and physics background, and using a simple four-vector smearing approach, yields promising results, and will be extended to fully simulated Monte Carlo events and eventually data.

A direct fit to the $m_{\text{top}}^{\text{reco}}$ distribution and the template method lead to different systematic uncertainties. An analysis is underway to systematically compare the two approaches. This is done for the $p_{\text{T-max}}$ and for a selection method that defines the top-quark as the jet triplet with the minimum sum of the three ΔR values.

Concerning the cross-section measurement an initial investigation of a cut and count analyses with and without using b-jet identification has been performed [?]. It exploits the lepton+jets channel at $\sqrt{s} = 10 \text{ TeV}$ and for $\mathcal{L}_{\text{int}} = 200 \text{ pb}^{-1}$. Within the systematic uncertainties investigated the total systematic uncertainty estimated is about 30%.

All-Jets Channel

In the all-jets channel only jet requirements and jet topologies can be used to separate the signal from the background reactions. Consequently, this channel suffers from a much higher background from the QCD multijet production. Here, events with isolated leptons are vetoed, and the missing transverse energy is required to be consistent with zero. In addition, at least six jets, not consistent with being purely electromagnetic, and two of which are identified b-jets, are required within $|\eta| < 2.5$. By exploring the transverse energies of the jets and the angular correlation of the two b-jets, the S/B is improved by several orders of magnitude to about 10^{-1} , while retaining a signal efficiency of about 10%. In this procedure the use of b-jet identification is absolutely essential. In addition, the availability of a multi-jet trigger with appropriate thresholds is imperative to not lose the signal events already at the trigger stage. This involves a delicate optimization to retain a sufficiently high efficiency for the signal events, while not saturating the ATLAS readout system with the QCD multijet events. The trigger conditions have been carefully studied, and the use of some trigger signals are suggested to ATLAS. Under the assumption that these will be available, and when exploiting the above event selection, a mass distribution has been isolated, where the signal starts to be visible on a still large background. For this analysis the next steps are the optimization of the background description and a fit to the distribution to access the sensitivity to m_{top} .

0.1.3 Searches for the Higgs Boson

The origin of particle masses is one of the most important open questions in particle physics. In the Standard Model, the answer to this question is connected with the prediction of a new elementary neutral particle, the Higgs boson H . The mass m_H of the Higgs boson is a free parameter of the theory. The experimental lower bound of 115 GeV has been set by the LEP experiments, while the recent searches at the Tevatron have excluded a SM Higgs boson in the mass range of $162 \text{ GeV} < m_H < 166 \text{ GeV}$. The theoretical upper limit of about 800 GeV still leaves a wide mass range to be explored.

In the minimal supersymmetric extension of the Standard Model (MSSM), the Higgs mechanism predicts the existence of five Higgs bosons, three neutral ($h/H/A$) and two charged ones H^\pm . Their production

cross sections and decays are determined by two independent parameters, e.g. the ratio $\tan\beta$ of the vacuum expectation values of the two Higgs doublets in this model and the mass m_A of the pseudoscalar Higgs boson. Current experimental searches at LEP and Tevatron exclude at a 95% confidence level the A boson mass values below 93 GeV, as well as the $\tan\beta$ values below 2. For an A boson mass of up to 200 GeV, also the high $\tan\beta$ values above 40 are excluded.

The search for the Higgs boson is one of the main motivations for the LHC and the ATLAS experiment. The high cross sections of the background processes exceeding the signal by many orders of magnitude call for selective triggers, efficient background suppression and reliable prediction of the background contributions. Until recently, the MPP group has been devoted to the preparation for an early Higgs boson discovery during the first years of LHC running at the nominal center of mass energy of 14 TeV. The results obtained in these studies can be found in the newly published review of the ATLAS physics potential [?]. As of lately, the searches are being optimized for the initial LHC operation at a center of mass energy of 7 TeV. With a relatively low expected total integrated luminosity of 1 fb^{-1} , the Higgs boson discovery is rather unlikely under these operating conditions. However, the allowed Higgs boson mass range can be constrained beyond the present experimental limits, as summarized in [?, ?].

The Standard Model Higgs Boson

The expected potential for the Standard Model Higgs boson discovery is shown in Fig. 15. In the mass range above 180 GeV, the key discovery channel is the Higgs boson decay into four charged leptons via two intermediate Z bosons. The lower mass range can only be covered by the combination of searches in several Higgs boson decay modes.

The clearest signature is found in the four-lepton decay channel $pp \rightarrow H \rightarrow ZZ^{(*)} \rightarrow 4\ell$ which also allows for a precise Higgs boson mass measurement. The reconstruction of this channel strongly relies on the high lepton identification efficiency and good momentum resolution of the ATLAS detector. The reducible $Zb\bar{b}$ and $t\bar{t}$ background processes can be suppressed by means of the Z boson mass reconstruction and the requirement of a low jet activity in the vicinity of each lepton. The remaining reducible background is small compared to the irreducible $pp \rightarrow ZZ^{(*)}$ background. In addition to the optimization of the analy-

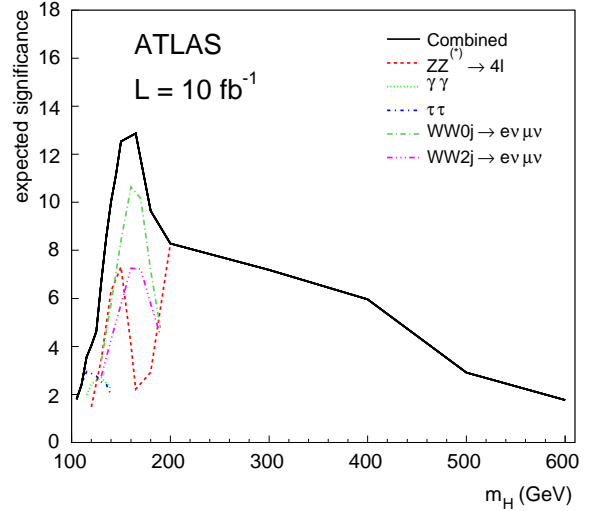


Figure 15: Discovery potential of the ATLAS experiment for the Standard Model Higgs boson. The statistical significance expected for an integrated luminosity of 10 fb^{-1} at a center of mass energy of 14 TeV is shown for the different Higgs boson decay modes and their combination as a function of the Higgs boson mass m_H . [?]

sis selection criteria, our studies include the detailed evaluation of the theoretical and experimental systematic uncertainties for both signal and background processes [?]. We also evaluate the potential to exclude a part of the allowed Higgs boson mass range in the initial phase of LHC operation [?], including the development of the methods for the precise determination of the background contributions from data. The expected exclusion limits are shown in Fig. 16 (top picture). The best upper limit on the Higgs boson production, obtained for the Higgs boson mass around 200 GeV, is still about a factor of two above the Standard Model prediction. The exclusion reach is especially low in the mass region around 160 GeV, where the $H \rightarrow ZZ^*$ decays are strongly suppressed by the Higgs boson decays into two on-shell W bosons.

Due to the high branching ratio for the decay $H \rightarrow W^+W^- \rightarrow (\ell^+\nu)(\ell^-\nu)$, the Higgs boson with a mass between 140 GeV and 180 GeV can be excluded in this channel during the initial phase of LHC operation. In combination with the four-lepton and the two-photon decay channels, the exclusion reach is slightly improved to cover the mass range from 135 GeV to 190 GeV, as shown in Fig. 16 (bottom picture). Due to the two neutrinos in the final state of the Higgs boson decays into W bosons, no precise measurement of the Higgs boson mass is possible. Precise determina-

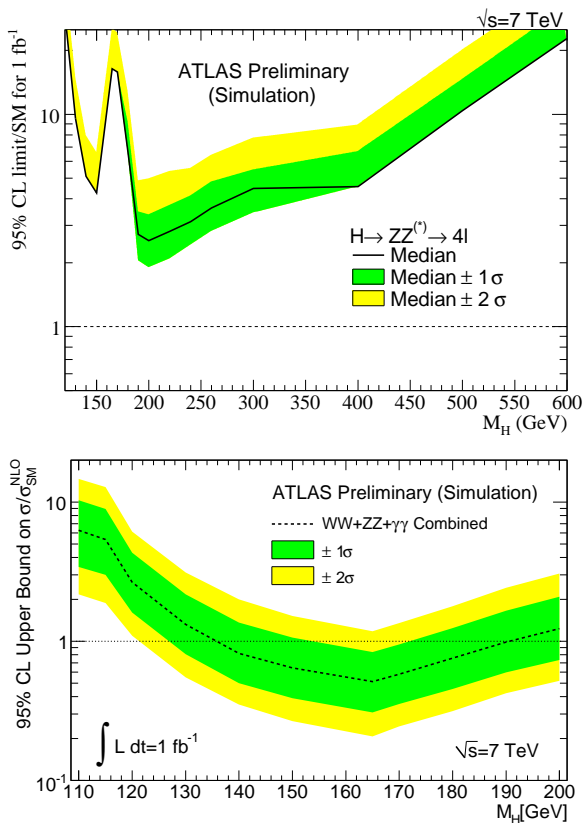


Figure 16: Expected upper limits (95% confidence level) on the Standard Model Higgs boson production rate in the $H \rightarrow ZZ^{(*)} \rightarrow 4\ell$ channel alone (top picture) and after the combination with the $H \rightarrow WW \rightarrow \ell\nu\ell\nu$ and $H \rightarrow \gamma\gamma$ channels (bottom picture). Both figures are shown as a function of the Higgs boson mass at an integrated luminosity of 1 fb^{-1} and a center of mass energy of 7 TeV, normalized to the Standard Model prediction. The bands indicate the 68% and 95% probability regions in which the limit is expected to fluctuate in the absence of signal. [?]

tion of the background contributions is therefore required to exclude the presence of signal events. For this purpose, we are measuring the Standard Model background processes with present LHC data. The $H \rightarrow WW$ decay channel also allows for an early Higgs boson discovery during the LHC operation at 14 TeV. Parallel to the optimization of the event selection criteria in this context [?], we have developed a new algorithm for the jet reconstruction [?, ?], which is used for the suppression of the $t\bar{t}$ and $W + jets$ backgrounds to the Higgs boson production via the W or Z gauge boson fusion. The algorithm reconstructs the jets using particle tracks in the inner detector instead of energy depositions in the calorimeters. The inner detector tracks can be associated to common vertices leading to a jet reconstruction probability which is in-

sensitive to the presence of multiple proton-proton interactions per beam collision (pile-up events).

In the mass range below 140 GeV, the Higgs boson predominantly decays into $b\bar{b}$ pairs. Due to the large contribution of QCD background in the gluon-fusion production mode, this decay can only be triggered and discriminated from the background in the production mode of the Higgs boson in association with a $t\bar{t}$ pair. Our studies have shown that the discovery potential in the $H \rightarrow b\bar{b}$ decay channel is very much limited by the large experimental systematic uncertainties [?, ?].

The second most frequent mode which can be observed in the mass range below 140 GeV is the decay into a $\tau^+\tau^-$ pair. This decay can only be discriminated against the background processes in the Higgs boson production mode via the W or Z gauge boson fusion where two additional forward jets in the final state provide a signature for background rejection. The decay modes with both τ leptons decaying leptonically ($\ell\ell$ mode) as well as with one hadronic and one leptonic τ -decay (lh mode) have been studied [?, ?]. The event selection criteria have been optimized using multivariate analysis techniques. With a neural network based background rejection method, the signal significance is improved compared to the standard analysis with sequential cuts on the discriminating variables, as shown in Fig. 17.

Higgs Bosons Beyond the Standard Model (MSSM)

The searches for the three neutral Higgs bosons predicted by the MSSM differ to some extent from the searches for the SM Higgs particle. Compared to the Standard Model, the neutral Higgs boson decay modes into two intermediate gauge bosons are suppressed in the MSSM, while the A and H boson decays into charged lepton pairs, $\mu^+\mu^-$ and $\tau^+\tau^-$ are enhanced. The later decay channel has an about three hundred times higher branching ratio compared to the first one but is more difficult to reconstruct and provides a less precise determination of the Higgs boson mass.

Our studies of MSSM Higgs boson decays into two τ leptons are summarized in [?]. The dominant background contribution originates from the $Z \rightarrow \tau^+\tau^-$ and $t\bar{t}$ processes and can be suppressed by the requirements on the presence of b jets in the final state and large angular separation between the two decaying leptons. This channel provides the highest sensitivity reach for the neutral MSSM Higgs bosons.

Motivated by the excellent muon reconstruction in the ATLAS detector, we also study the prospects for

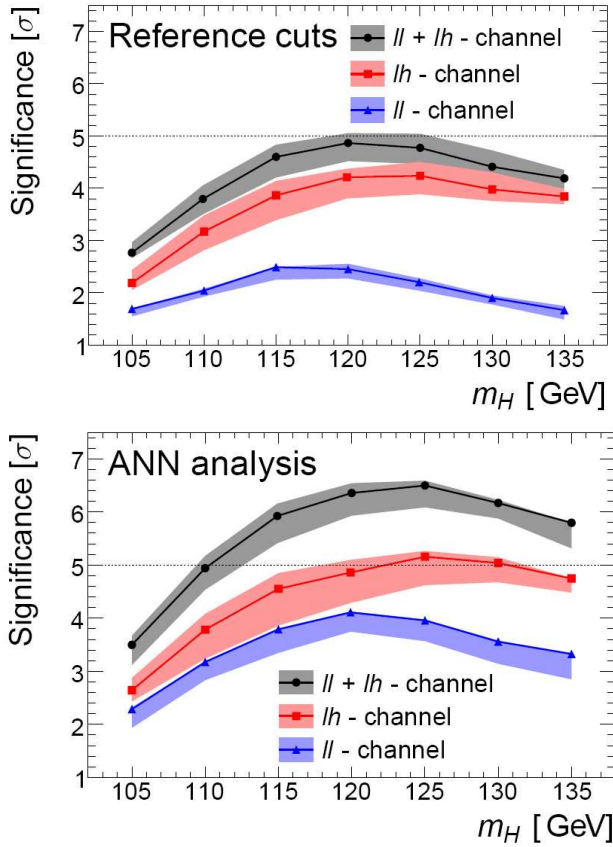


Figure 17: Discovery potential for the Higgs boson search in the $H \rightarrow \tau^+\tau^-$ decay channel, shown separately for the ll and lh decay modes and their combination at an integrated luminosity of 30 fb^{-1} and a center of mass energy of 14 TeV. The results are obtained using the standard analysis with sequential cuts on the discriminating variables (top picture), as well as for neural network based analysis (bottom picture). The shaded bands indicate the effect of the experimental systematic uncertainties. [?]

the search in the channel with MSSM Higgs boson decays into two oppositely charged muons. The event selection criteria are optimized for the best discovery potential taking into account the theoretical and experimental systematic uncertainties [?]. The invariant dimuon mass distribution after all analysis selection criteria is shown for the signal and dominant background processes in Fig. 18. The dominant $Z \rightarrow \mu^+\mu^-$ and $t\bar{t}$ background contributions are rather large compared to the signal and are subject to sizable experimental systematic uncertainties, particularly with regard to the jet energy scale. It is therefore important to measure this background contribution with data. This can be done by combining the information from the side-bands of the invariant dimuon mass distribution with the measurements on

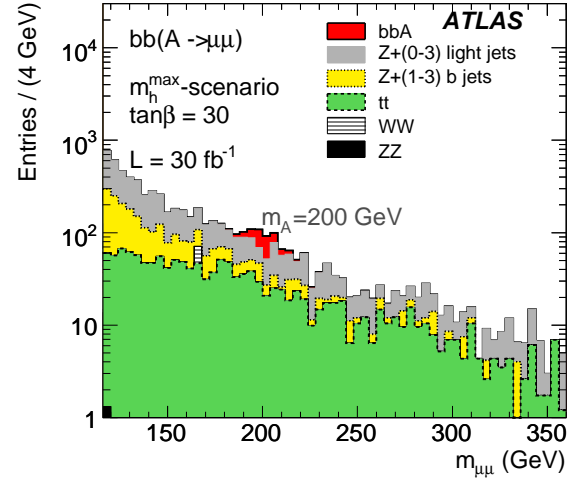


Figure 18: Invariant dimuon mass distributions of the main backgrounds and the A boson signal at mass $m_A = 200 \text{ GeV}$ and $\tan\beta = 30$, obtained for the integrated luminosity of 30 fb^{-1} at a center of mass energy of 14 TeV. Only events with at least one reconstructed b jet in the final state are selected. [?]

the e^+e^- control sample. The latter is motivated by an almost vanishing Higgs boson decay probability into two electrons, while the background contributions are similar for the dimuon and the dielectron final states. The expected ratio of invariant dielectron and dimuon mass distributions is shown in Fig. 19 after all analysis selection criteria and after correcting for the different electron and muon reconstruction and identification efficiency. We perform a detailed study of

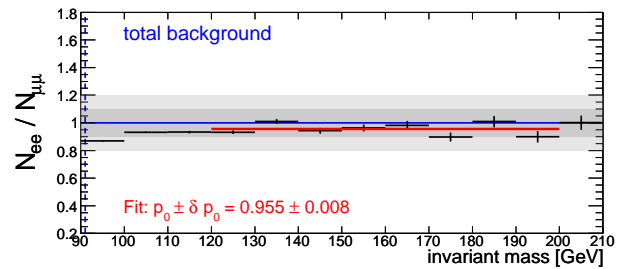


Figure 19: Ratio of the dilepton invariant mass distributions for the e^+e^- control sample and the total $\mu^+\mu^-$ background for the Higgs boson search in the $h/A/H \rightarrow \mu^+\mu^-$ channel, shown for an integrated luminosity of 4 fb^{-1} . [?]

the background estimation from data in [?, ?]. The presented method allows for a significant decrease of systematic uncertainties and thus in an improved sensitivity reach for the MSSM Higgs boson search in the $\mu^+\mu^-$ decay channel. Especially during the ini-

tial phase of LHC running with the limited amount of data, the introduced control data samples are essential for obtaining reliable exclusion limits. The exclusion reach with early data at a center of mass energy of 7 TeV has been evaluated for the $h/H/A \rightarrow \mu^+\mu^-$ channel in [?], see Fig. 20. At an integrated luminosity of 1 fb^{-1} one cannot improve the current limits reached by the Tevatron experiments using this channel alone. However, its combination with searches in a more sensitive $h/H/A \rightarrow \tau^+\tau^-$ decay channel allows for an improved coverage of the $(m_A, \tan\beta)$ parameter space.

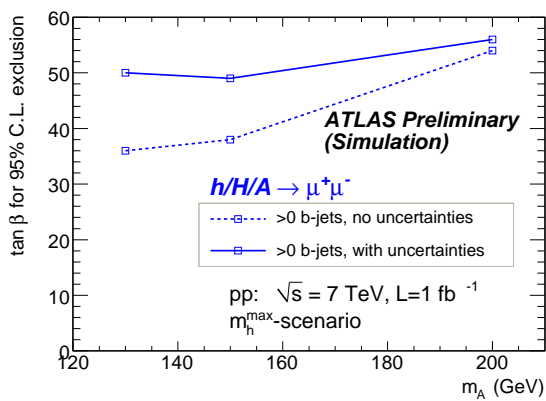


Figure 20: The $\tan\beta$ values needed for an exclusion of the neutral MSSM Higgs bosons shown as a function of the Higgs boson mass m_A for the analysis mode with at least one b-jet in the final state. An integrated luminosity of 1 fb^{-1} and a center of mass energy of 7 TeV are assumed. Dashed lines represent the results assuming zero uncertainty on the signal and background, while the full lines correspond to the results with both signal and background uncertainty taken into account. [?]

The light neutral MSSM Higgs boson is difficult to distinguish from the Standard Model Higgs boson. Clear evidence for physics beyond the Standard Model would be provided by the discovery of charged scalar Higgs bosons. We have studied the prospects for the search for the charged MSSM Higgs bosons in the decay channel $H^\pm \rightarrow \tau^\pm\nu_\tau$ which dominates for relatively small Higgs boson masses below 200 GeV [?, ?]. The charged Higgs bosons are produced in top quark decays in $pp \rightarrow t\bar{t} \rightarrow (bH^\pm)(bW^\mp)$ events. The τ leptons from H^\pm decays are reconstructed in their hadronic decay modes while the W bosons from top quark decays are required to decay leptonically. Since H^\pm mass cannot be reconstructed because of the undetected neutrinos in the final state, these events can only be distinguished as an excess of events with recon-

structed τ leptons and large missing transverse energy above the high background of standard model decays of top quark pairs. In Fig. 21, the discovery region in the $(m_{H^\pm}, \tan\beta)$ plane is shown for a charged Higgs boson in the above production and decay mode assuming different amounts of integrated luminosity. The theo-

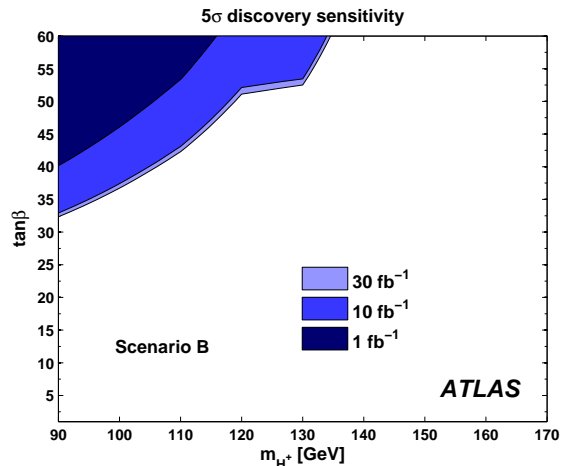


Figure 21: The $\tan\beta$ values needed for a discovery of the charged MSSM Higgs bosons shown as a function of the Higgs boson mass m_{H^\pm} for different levels of integrated luminosity. A center of mass energy of 14 TeV is assumed. The decays $H^\pm \rightarrow \tau^\pm\nu_\tau$ can be discovered with at least 5 σ significance in all shaded regions of the parameter space. [?]

retical and experimental systematic uncertainties have been taken into account. We have developed the methods to decrease the original instrumental background uncertainty of 50% down to 10% by means of the control measurements on data [?, ?].

0.1.4 Search for Physics Beyond the Standard Model

Supersymmetric Particles

Supersymmetry (SUSY) is the theoretically favored model for physics beyond the Standard Model. The new symmetry uniting fermions and bosons predicts for each Standard Model particle a new supersymmetric partner with the spin quantum number differing by $1/2$. Supersymmetry provides a natural explanation for Higgs boson masses near the electroweak scale. In addition, the lightest stable supersymmetric particle is a good candidate for the dark matter. The SUSY models can also provide solutions to the problem of the unification of the fundamental forces. In order to suppress the SUSY-induced processes violating the baryonic and leptonic quantum numbers, the so-called

R-parity has been introduced as a conserved quantum number. Each SM particle has an R-parity equal to 1, while the supersymmetric partners carry an opposite sign, i.e. an R-parity of -1.

If the mass scale of the SUSY particles is accessible at the LHC, the squarks and gluinos (the superpartners of quarks and gluons with spin 0 and 1/2, respectively) will be copiously produced in pp collisions. Assuming that the R-parity is conserved in these processes, all supersymmetric particles must be produced in pairs and each will decay to the weakly interacting lightest supersymmetric particle via decay chains involving the production of quarks and leptons. Therefore, the SUSY events at the LHC are characterized by the large missing transverse energy, highly energetic jets and leptons.

If the supersymmetry would be a conserved symmetry, each particle and its superpartner are expected to have an equal mass. However, since the supersymmetric partners of the Standard Model particles are not observed so far, SUSY must be a broken symmetry. A model with the SUSY breaking mechanism mediated by the gravitational interaction is called mSUGRA and is described by the common mass terms m_0 and $m_{1/2}$ for all boson and fermion masses, respectively, at an energy scale above 10^{15} GeV, where the electroweak and strong interactions are unified (GUT scale).

The searches for SUSY signatures with conserved R-parity are performed in ATLAS by searching for an excess of events in various channels. These channels explore a large variety of possible signatures in the detector, divided according to different jet and lepton multiplicities. Fig. 22 shows the 5σ discovery reach for the mSUGRA model in the final states with 4 jets and 0 leptons, the states with 4 jets and 1 lepton or in the final states with 2 jets and 2 leptons.

The Standard Model processes with similar signatures as the signal are the top-quark pair ($t\bar{t}$) and the gauge bosons (W and Z) production. These processes are characterized by a large missing transverse energy originating from weakly interacting neutrinos and therefore constitute the main background to SUSY searches at the LHC. Additional important source of the background is the QCD jet production in which the mis-measured jet energy can lead to the high-energy tails in the distribution of the missing transverse energy. It is expected that at the LHC the Monte Carlo prediction will not be sufficient to achieve the good understanding and the control of the background for the SUSY searches. Our studies are concentrating on the

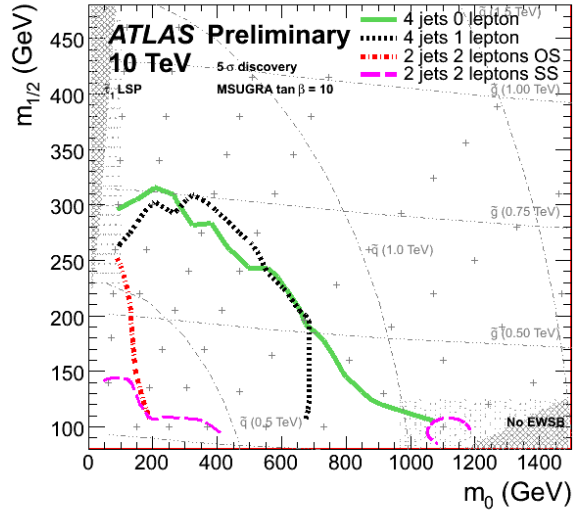


Figure 22: The 5σ discovery reach of the ATLAS experiment in the search for the mSUGRA signal using channels with various jet and lepton multiplicities in the $(m_0, m_{1/2})$ parameter space of the mSUGRA model. The discovery reach is evaluated for the center of mass energy of 10 TeV and an integrated luminosity of 200 pb^{-1} .

data-driven estimation of these, which is essential for an early discovery of SUSY with the ATLAS detector.

We have developed the methods for the determination of the $t\bar{t}$ background contribution from data [?]. The background contribution is measured by means of the control data samples which are free of the SUSY signal contribution. The contribution from the $t\bar{t}$ production with top quark decays involving the τ leptons and non-reconstructed electrons or muons is estimated from similar events with identified muons and electrons. The control data sample is composed mainly of $t\bar{t}$ events in which both top quarks decay into a b-quark, neutrino and a lepton (electron or muon). Additional kinematic constraints are applied on these events similarly to the criteria used for the signal selection. The number of b-jet pairs passing the kinematic constraints is used to divide the measured data sample into the SUSY-dominated and the $t\bar{t}$ -dominated region (see Fig. 23).

Similar strategy is used to define the control sample with semi-leptonic $t\bar{t} \rightarrow (\ell\nu b)(q\bar{q}b)$ decays [?]. In this case the discriminating variable distinguishing between the signal and the background region is the invariant mass of the three nearby jets. In case of the $t\bar{t}$ events, the value of this variable will be close to the top quark mass (see Fig. 24).

The contribution of the $t\bar{t}$ background with tau lep-

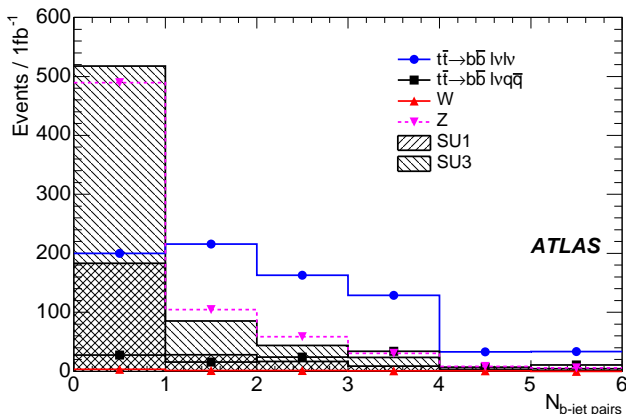


Figure 23: Number of b-jet pairs $N_{b\text{-jet pairs}}$ selected after the kinematic constraints on the $t\bar{t} \rightarrow (\ell\nu b)(\ell\nu b)$ process. The $N_{b\text{-jet pairs}} > 0$ region is mainly populated by the $t\bar{t}$ events. This region is used as a control data sample for the estimations of the $t\bar{t}$ background to the searches for SUSY signatures with one lepton in the final state. The events with $N_{b\text{-jet pairs}} = 0$ originate predominantly from the gauge boson production processes and by the SUSY signal. The two typical SUSY models labeled SU1 and SU3 are shown for the signal. [?]

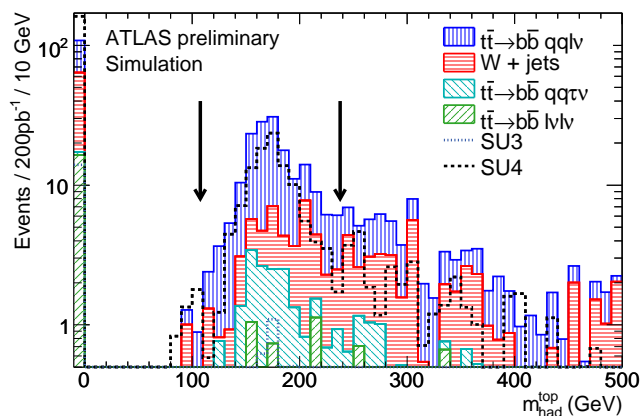


Figure 24: Invariant mass of the tree nearby jets in each event. This variable is used for the selection of the control data sample of $t\bar{t} \rightarrow (\ell\nu b)(qqb)$ events, needed for an estimation of the $t\bar{t}$ background in SUSY searches with no-lepton signatures. The arrows indicate the selected window for this variable. The contributions of the Standard Model processes are shown by the stacked hatched histograms. The SUSY contribution for two typical SUSY mSUGRA models (SU3 and SU4) are overlaid. [?]

tons produced in top-quark decays can be estimated from the control data sample by replacing the reconstructed electron or muon with a simulated tau lepton decay (see Fig. 25). Similarly, one can also estimate the contribution of $t\bar{t}$ with a non-identified electron

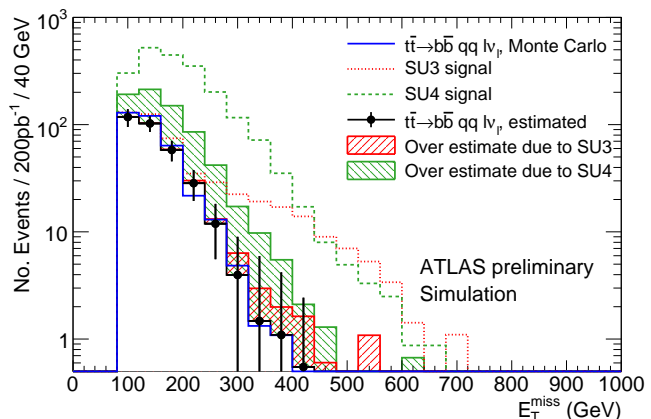


Figure 25: Missing transverse energy distribution in the one-lepton final state. The solid line shows the Monte Carlo estimate, circles are the result of data-driven estimation. The shaded histograms show the increase of the data-driven estimates due to the contaminating SUSY signal (represented by SU3 and SU4 models) in the control data sample and the dashed lines show the SUSY signals stacked on the top of the $t\bar{t}$ background. [?]

or muon by removing the reconstructed leptons from each event in the control data sample.

We analyzed a set of the most important kinematic variables for the 70 nb^{-1} of data collected by the ATLAS experiment [?]. We find a good agreement between data and Monte Carlo predictions, indicating that the Standard Model backgrounds for the SUSY searches are well under control (see Fig. 26).

Other Extensions of the Standard Model

The discovery of the neutrino flavour oscillations has shown that the lepton flavour is not a conserved quantity within the Standard Model. Beyond the SM, the lepton flavour violation can occur in many SUSY extensions. One of the lepton flavour violating process accessible at the LHC is a neutrinoless decay of a tau lepton $\tau \rightarrow \mu\mu\mu$. Although the Standard Model predicts a very small branching ratio for this decay, $\mathcal{BR}(\tau \rightarrow \mu\mu\mu) \leq 10^{-14}$, some extensions of the Standard Model, such as SUSY and models with doubly charged Higgs boson, predict the values which are several orders of magnitude higher. Therefore, the measurement of the branching ratio for the $\tau \rightarrow \mu\mu\mu$ decay will put stringent limits on the parameters of such models beyond SM.

During one year of data-taking at the low luminosity of $10^{33} \text{ cm}^{-2}\text{s}^{-1}$, ATLAS will collect 10^{12} τ lepton decays. Due to the very large background contribu-

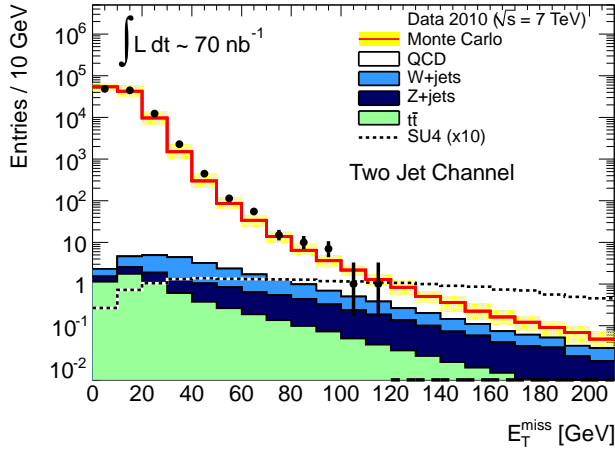


Figure 26: Distribution of missing transverse energy in the two-jets final state. Black points show the measurement results with 70 nb^{-1} of data collected by the ATLAS experiment. Shaded histograms show the contribution from the gauge boson and top-quark production processes. The open red histogram is the QCD di-jet production process. The prediction of the low-mass mSUGRA model SU4 (enhanced by a factor of 10) is shown by a black dashed line. [?]

tion only a fraction of these decays can be observed in ATLAS, namely the decays of τ leptons originating from the W and Z boson decays. We studied the sensitivity of the ATLAS detector to the $\tau \rightarrow \mu\mu\mu$ decay, where the tau lepton is produced in the decay of W boson [?]. This process is characterized by a large missing transverse energy from the non-detectable neutrino and by the three nearby muon tracks. The main background processes are the production of charmed and beauty mesons, with their subsequent decays into muons (see Fig. 27).

The study with the simulated data shows that the upper limit of $\mathcal{BR}(\tau \rightarrow \mu\mu\mu) \leq 5.9 \cdot 10^{-7}$ can be achieved with 10 fb^{-1} of collected data. Extrapolating this expected sensitivity to higher integrated luminosities, an integrated luminosity of 100 fb^{-1} has to be collected by the ATLAS experiment to reach the current best upper limit of $\mathcal{BR}(\tau \rightarrow \mu\mu\mu) \leq 3.2 \cdot 10^{-8}$ (90% CL) by the BELLE experiment.

In addition to the described study of the lepton flavour violation, we pursue the searches for non-Standard Model heavy neutral gauge boson Z' . This particle is predicted by some extensions of the Standard Model which address the problems of the mass hierarchy and the number of generations of lepton and quarks.

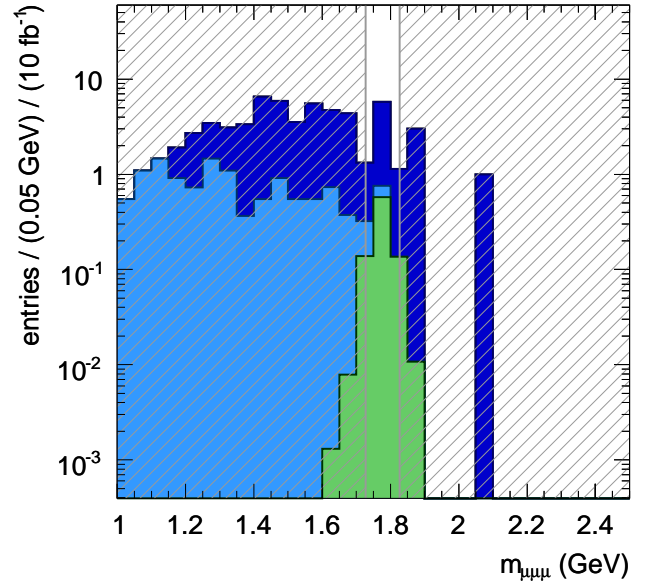


Figure 27: Invariant mass distribution of the tree nearby muons, shown for the signal and background processes after applying all analysis selection criteria. The signal consists of the $\tau \rightarrow \mu\mu\mu$ decays with tau leptons originating from the W bosons (green), while the background processes include the decays of charmed and beauty mesons. Histograms are normalized to an integrated luminosity of 10 fb^{-1} at a center of mass energy of 14 TeV . Non-shaded area represents the selected mass window for the evaluation of the limits on the branching ratio. [?]

0.1.5 Analyses Summary

In summary the MPP physics analyses are well advanced. First measurements of the inclusive lepton distributions and of the electroweak gauge boson production have recently been performed. A variety of paths are explored in the search for the most appropriate variable and analysis strategy to determine the top-quark mass, a measurement that will soon be dominated by the systematic uncertainty. In the context of the searches for new physics phenomena, many new methods have been developed to understand the background contribution originating from the above SM processes. Strategies for the Higgs boson and supersymmetry searches are optimized for the highest possible sensitivity during the early data taking phase. Members of the group are actively participating in the ATLAS efforts and have presented their own and the ATLAS collaboration results at international conferences [?, ?, ?, ?, ?, ?, ?, ?].

Juli 2010

Alle Rechte vorbehalten

Max-Planck-Institut für Physik (Werner-Heisenberg-Institut), München
(edited by S. Stojek)